SAND74-0378
Unlimited Release

Nonlinear Stress Analysis of Vertical-Axis Wind Turbine Blades

L. I. Weingarten, R. E. Nickell

Prepared by Sandia Laboratories, Albuquerque, New Mexico 87115 and Livermore, California 94550 for the United States Energy Research and Development Administration under Contract AT(29-1)-789

Printed April 1975

When printing a copy of any digitized SAND Report, you are required to update the markings to current standards.

Sandia Laboratories
energy report

SF 2900-QQB(3-74)

Issued by Sandia Laboratories, operated for the United States Atomic Energy Commission by Sandia Corporation.

NOTICE

This report was prepared as an account of work sponsored by the United States Government. Neither the United States nor the United States Atomic Energy Commission, nor any of their employees, nor any of their contractors, subcontractors, or their employees, makes any warranty, express or implied, or assumes any legal liability or responsibility for the accuracy, completeness or usefulness of any information, apparatus, product or process disclosed, or represents that its use would not infringe privately owned rights.

SF 1004-DF(2-74)

SAND74-0378

Nonlinear Stress Analysis of Vertical-Axis Wind Turbine Blades†

L. I. Weingarten*

R. E. Nickell**

A Darrieus type vertical-axis wind turbine with a "troposkien" blade shape has been proposed by Sandia Laboratories as an alternate to conventional horizontal axis, propeller-type machines. The troposkien (Greek for turning rope) shape eliminates blade bending and thereby results in a more efficient, minimum material blade design. Manufacturing considerations have resulted in a prototype blade shape that deviates slightly from the troposkien shape. The effect on the stress distribution of this alternate blade shape is investigated. Analytical models of the blades were constructed using a general purpose, nonlinear, dynamic finite element structural code. This code accounts for the large deflection effects of the various blade shapes through incremental applications of angular velocity.

†This work was supported by the U.S. Energy Research and Development Administration.

* Engineering Analysis Department, Sandia Laboratories, Albuquerque, N.M. 87115, Associate Member ASME.

** Engineering Analysis Department, Sandia Laboratories, Albuquerque, N.M. 87115, Member ASME.

Introduction

In fiscal year 74, Sandia Laboratories commenced a study of the Darrieus type vertical-axis wind turbine. This type of wind turbine is proposed as an alternative to conventional horizontal axis, propeller-type machines. An advantage is that the blades, if properly designed, will be primarily in tension, thus tending toward more efficient structural behavior. In connection with its vertical-axis wind turbine program, Sandia Laboratories has developed the troposkien shape for the blade design. This shape, shown in Fig. 1 by the dashed line, is derived in Ref. 1 assuming a perfectly flexible blade under the action of centrifugal forces only. In order to facilitate the fabrication of a prototype and in order to reduce costs, the blade is in fact made of two straight members pinned to a center circular member. All members represent symmetric airfoils in cross sections. The straight members are airfoils composed of low carbon steel bent to the desired shape. The circular arc has a low-carbon steel strip for a backbone encased in foam. Its cross-sectional shape is that of a NACA 0012 airfoil. The prototype, presently being tested at Sandia Laboratories, has three blades of the type described above. This is shown in Figure 2.

The effect on the stress distribution of an alternate blade shape to that of the troposkien is investigated. Primary concern is with the variation in stress from the pure tensile state. As with all problems involving rotating machinery, the system natural frequencies are also of importance. The ability of this type of flexible structure to support acceleration loads depends upon nonlinear geometrical adjustments as the angular velocity is increased. An analytical model of this behavior was constructed using a general purpose, nonlinear, dynamic finite element structural code. This code accounts for the large deflection effects through incremental applications of angular velocity. A beam-type solution is also obtained for the stresses in the straight section, which can be used to validate the finite element analyses or as an additional, less expensive, design tool.

Analytical Methods

Reference analyses of the turbine blades were carried out with a general purpose, nonlinear finite element program. The basic element chosen from the element library of this program was a two-node, isoparametric, curved beam element with bending in one plane only. The geometric description for each element

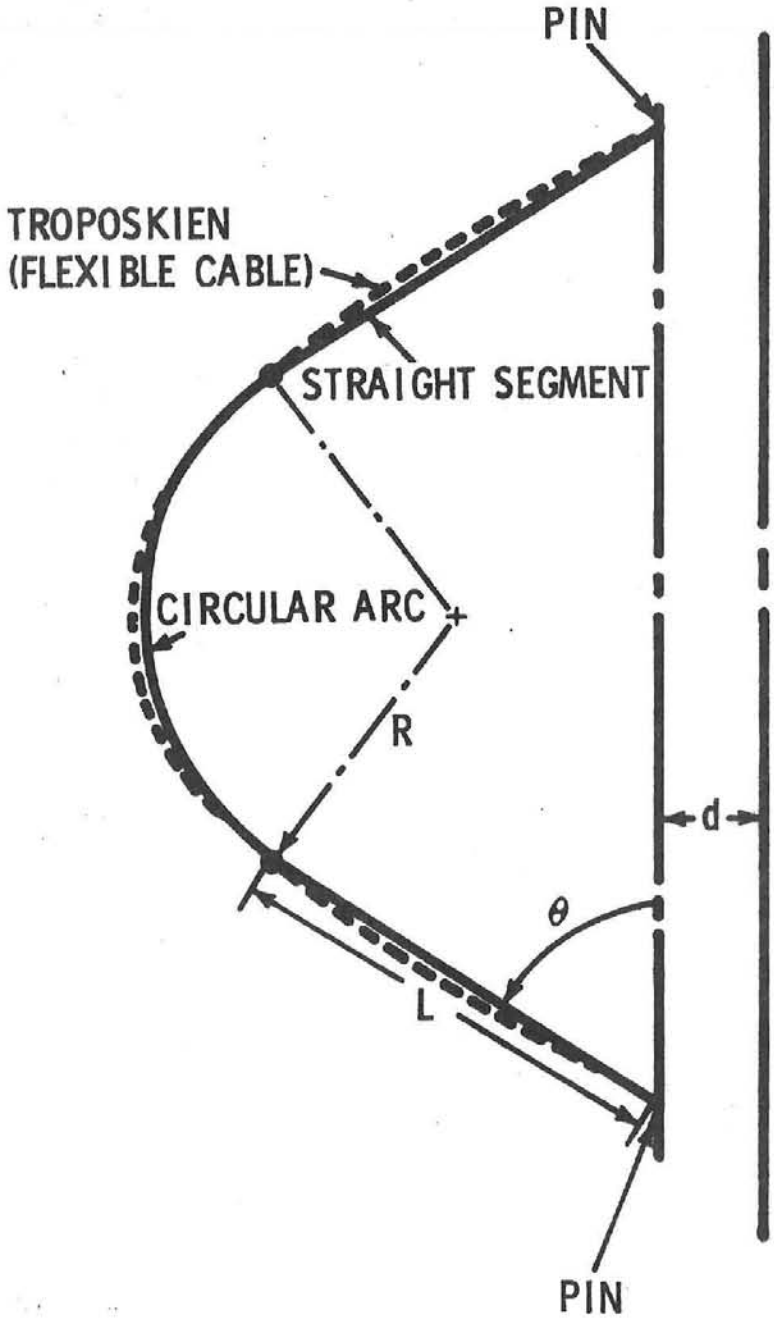

FIGURE 1. Blade Geometry.

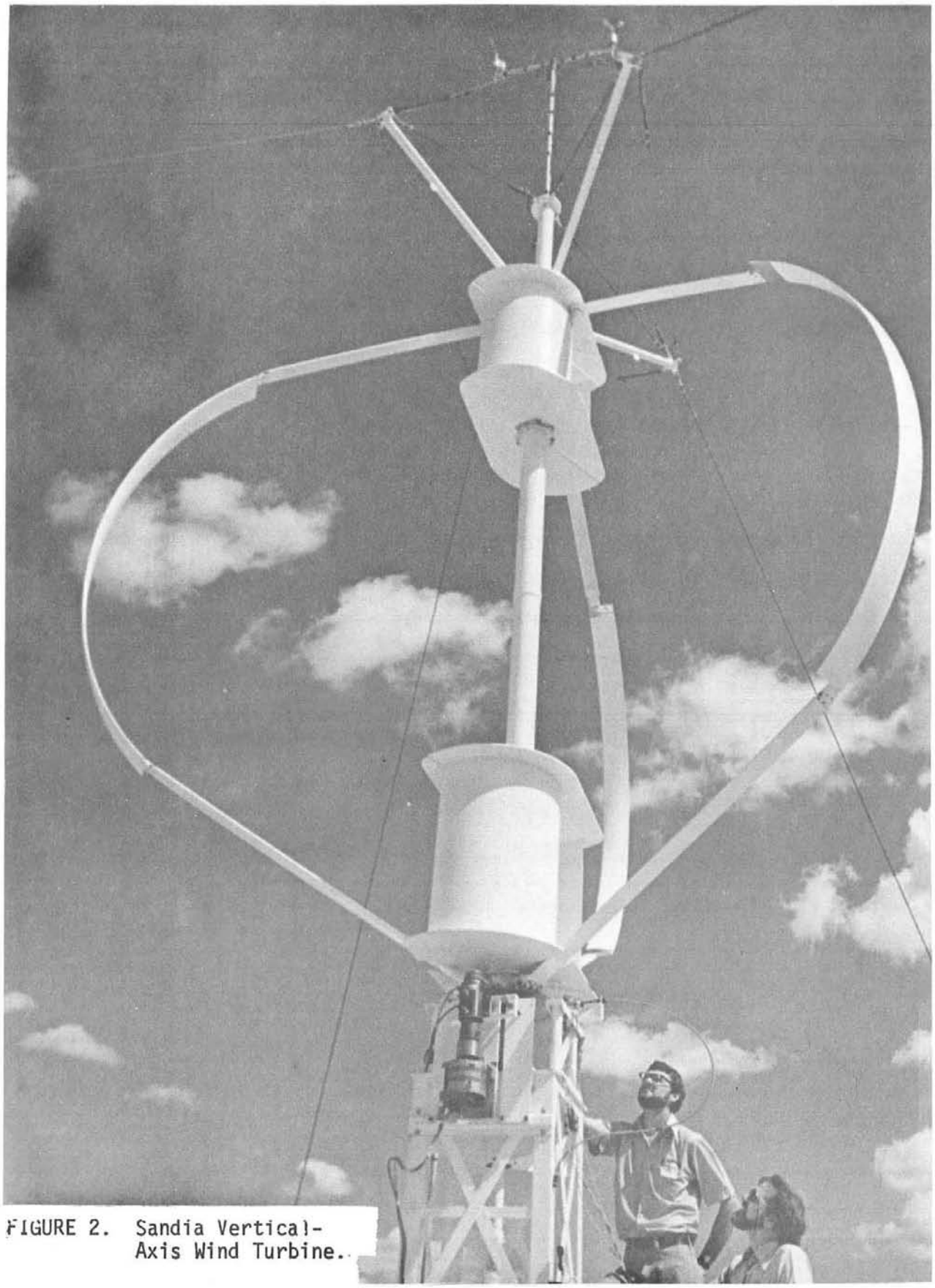

FIGURE 2. Sandia Vertical-Axis Wind Turbine.

requires five coordinates for each nodal point: the x and y coordinates; the distance, s, measured along the reference surface of the beam, with respect to an arbitrary starting point; and the derivatives dx/ds and dy/ds.

Both the in-plane and transverse displacement fields, u and w, are expanded into cubic polynomials in s; the unknown coefficients are the nodal point displacements and the derivatives du/ds and dw/ds at the nodes. Element mass and stiffness matrices are calculated through approximate (Gaussian) volume integration of inertial and strain energy expressions, with five Gauss points used along the length of each beam element. Eleven integration points are specified through the thickness.

The element is discussed in more detail in [2]. Its principal attribute appears to be a high rate of convergence, even for geometrically nonlinear problems, due to an ability to "represent exactly all of the rigid body modes of the interpolated surface" [3].

Geometrically nonlinear effects are treated as in [4]. The loading, in this case, is centrifugal acceleration and, theoretically, such loads would be nonconservative (large rotations will affect the distribution of mass in the structure). A Lagrangian reference frame is employed here, however, and since the rotations are limited to about one degree at angular velocities of 40 rad/sec maximum, the conservative treatment of the loads is not felt to be seriously in error.

An incremental application of these acceleration loads gives the structure (through the tangent stiffness matrix, which is recomputed after each load step) an opportunity to adjust its shape for better load-carrying capacity. Within each load step, a modified Newton-Raphson procedure is adopted--the solution is iterated, with the tangent stiffness matrix remaining as computed at the beginning of the step, until the incremental displacements converge to some specified tolerance.

Occasionally, within a series of load steps, the first few natural frequencies of the deformed structure may be of interest. When such information is needed, the incremental loading is halted temporarily and the tangent stiffness associated with the current deflected shape is computed; the consistent mass matrix is also computed; and a specified number of the lower mode shapes and frequencies are found through inverse iteration [5].

The idealization of the structure for the finite element code is as follows. The straight sections contained 10 elements and the circular arc section contained 20 elements. The pin between the straight and circular section was represented

by an element of low bending stiffness. The circular arc section is designed so that the steel backbone carries all the load. The other pertinent parameters used in the analysis are:

$\rho = 7.332 \times 10^{-4} \frac{\text{lb+sec}^2}{\text{in}^4}$ (7834 kg/m^3) = mass density

$d = 5.5''$ (.1397 m) = radius of shaft about which blade rotates

$R = 57.6318''$ (1.4638 m) = radius of circular section

$L = 73.07335''$ (1.8561 m) = length of straight section

$\theta = 57.25^{\circ}$ = angle subtended by straight section and shaft

$E = 30 \times 10^6$ psi (2.07×10^{11} Pa) = Young's modulus

$I_s = .05836$ in^4 (2.4291×10^{-8} m^4) = bending moment of inertia

$I_c = .0004883$ in^4 ($.02032 \times 10^{-8}$ m^4) = bending moment of inertia

$A_s = .765$ in^2 (4.935×10^{-4} m^2) = cross-sectional area

$A_c = .375$ in^2 (2.419×10^{-4} m^2) = cross-sectional area

The subscripts s and c pertain to the straight and circular sections, respectively. The rotational velocity of the wind turbine, Ω, was varied to an upper limit of 40 rad/sec since this was approximately the highest expected and observed during operation. A weight of 5 lb (2.268 kg) was added to the elements between straight and circular sections to account for knuckles at these locations. For similar reasons, 3 lb (1.3608 kg) was added adjacent to the pins at the shaft.

Results

Figure 3 shows the deflected shape of the blade when spun at 40 rad/sec. The original configuration is to scale and the deflections are magnified by a factor of 10. The straight sections can be seen to swing out and bend. This, combined with the high centrifugal forces on the center section, induces significant bending within the circular section.

In Figure 4, the bending stresses at the inner and outer fibers of the blade are plotted versus the ratio of s to S, the half-blade length. The highest stresses occur in the straight member at $s/S \approx .37$. This outer fiber stress is plotted versus turbine speed in Figure 5. The highest stresses of approximately

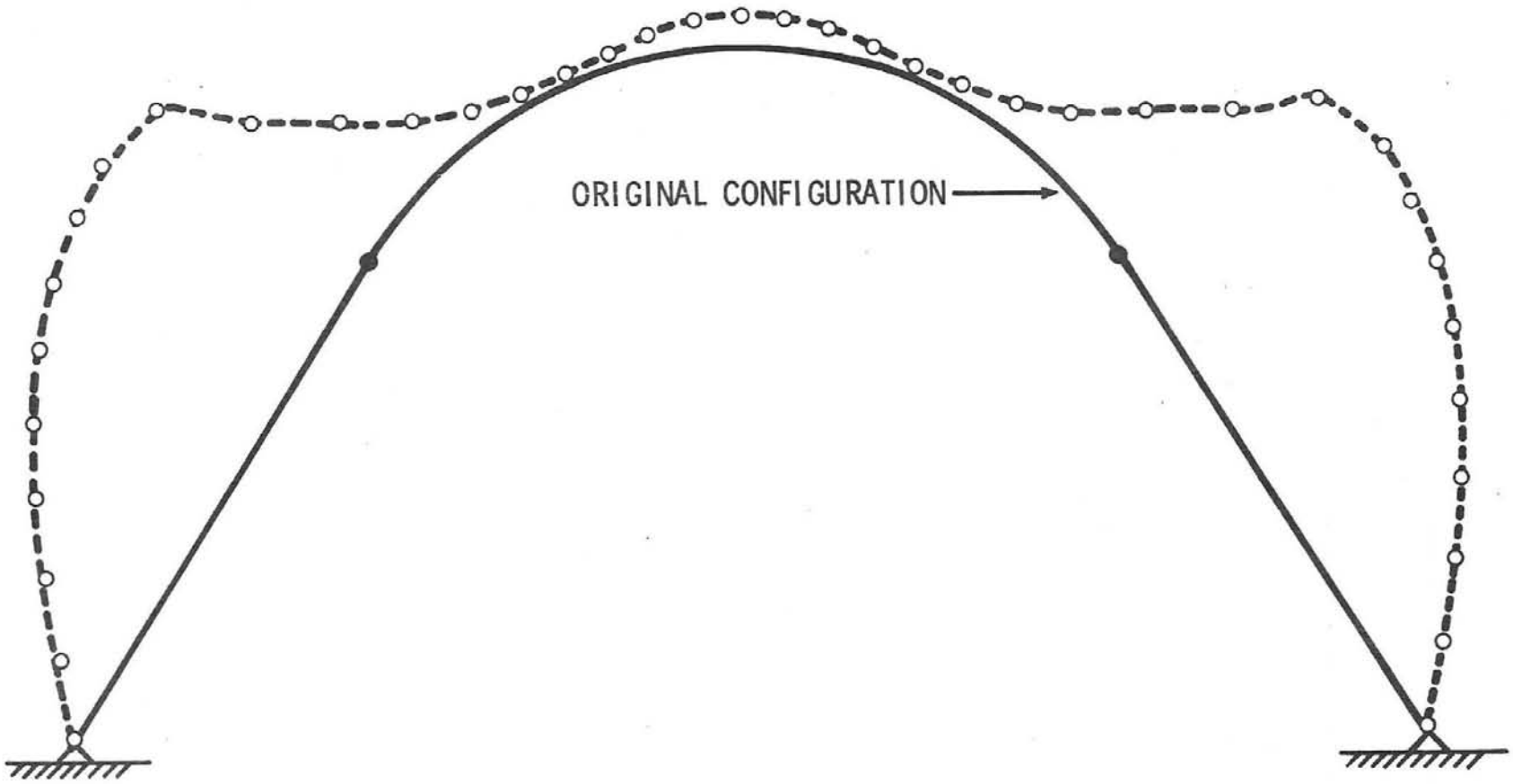

FIGURE 3. Deflected Shape (10X) of Blade at Ω = 40 Rad/Sec.

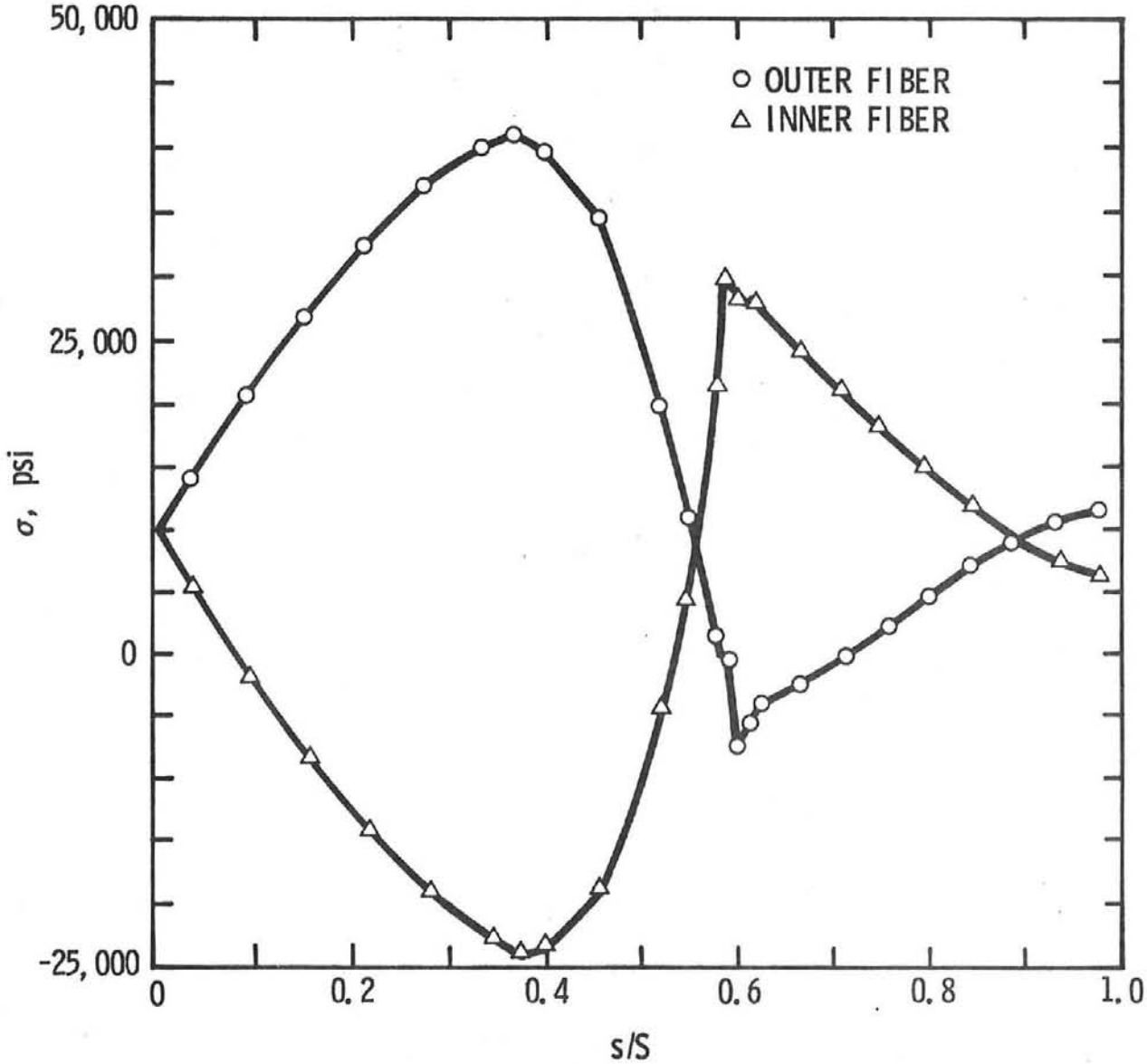

FIGURE 4. Meridional Stress, σ, vs. Meridional Coordinate, s/S.

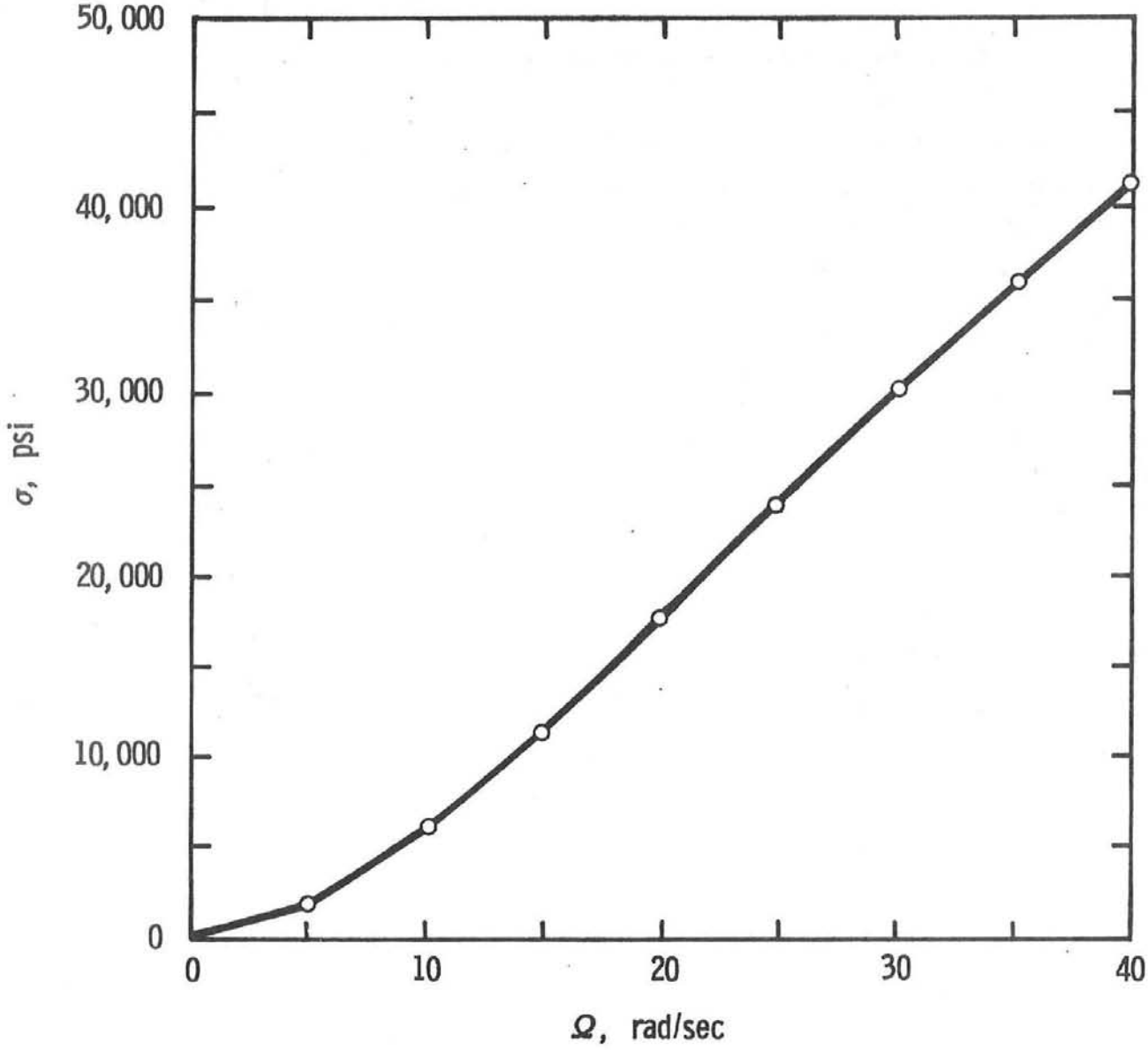

FIGURE 5. Outer Fiber Meridional Stress, σ, vs. Angular Velocity, Ω at s/S = .37. (This is maximum stress at high angular velocities.)

40000 psi (2.7579×10^8 Pa) are higher than the yield stress of the low-carbon steel used, 35000 psi (2.4132×10^8 Pa), indicating that a small amount of yielding should take place. Upon examination of the straight sections in the prototype, this was verified. There was a small permanent deflection in the beam with a maximum at $s/L \approx .7$.

In order to verify the results of the finite element code and to provide a design tool for those without access to large structural codes, the following beam analysis is provided. Since, in general, the maximum stress occurs in the straight sections, the analysis will focus on these members. The blade is assumed to be under a constant tension. For the purposes of the numerical example to follow, this is specified to be equal to the average of the tension predicted by the finite element code. The results obtained by a troposkien analysis (Ref. 1) could also be used to calculate this tension. The results are very nearly identical. If the deflections are assumed to be small and linear elasticity with no shearing deformations is adopted, the equilibrium equation is [6]

$$EI_s \frac{d^2w}{ds^2} = M = Tw + M_q \tag{1}$$

where M = bending moment,

M_q = bending moment due to a distributed load per unit length q

T = tensile force

w = deflection normal to straight member

The loading, q, is the component of the centrifugal loading per unit length perpendicular to the beam axis

$$q = \rho A_s \Omega^2 \, (s \sin\theta + d) \cos\theta \tag{2}$$

The boundary conditions for a pinned beam are:

$$w = M = 0 \quad @ \quad s = 0, L$$

The meridional stress, σ, at the outer and inner fibers of the beam can then be found to be

$$\sigma \; \frac{T}{A_s} \mp \frac{Eh_s}{2T} \rho A_s \Omega^2 \left\{ L \sin\theta \left[\frac{\sinh\alpha x}{\sinh\alpha L} - \frac{x}{L} \right] + d \left[\frac{\cosh\alpha(\frac{L}{2} - x)}{\cosh\alpha \frac{L}{2}} - 1 \right] \right\} \cos\theta \tag{3}$$

where $\alpha^2 = T/EI_s$

h_s = effective thickness of straight member

Figure 6 shows the maximum resultant stress in the straight section as calculated by the simple beam and finite element solutions. The small differences can be attributed to two points: (1) the tension, in fact, varies along the length and (2) large deflection effects were neglected in the simple beam analysis.

It should be noted that, when the blade was modeled as a troposkien, the finite element code confirmed the results of Ref. 1. The blade was essentially in pure tension with a maximum tensile stress of approximately 10000 psi ($.6895 \times 10^8$ Pa) at Ω = 40 rad/sec.

The possibility of forced resonance due to a congruence of turbine blade angular velocity and blade natural frequency was also investigated. A typical result is shown in Fig. 7, where the first two natural frequencies and their associated mode shapes are given for a blade angular velocity of 40 rad/sec. By contrasting the mode shapes with the undeformed shape, the first mode (~65 rad/sec) is seen to be antisymmetric with respect to the y-axis; the second mode (~110 rad/sec), on the other hand, is symmetric. To the designer, a more telling point can be made with Fig. 8, where the natural frequencies for these two modes are plotted against blade angular velocity. The line of congruence is shown by a solid line; should either of the two frequency curves cross this line, the corresponding Ω would represent an angular velocity to be scrupulously avoided during turbine operation. From Fig. 8, there would appear to be no such design limitation for this structure.

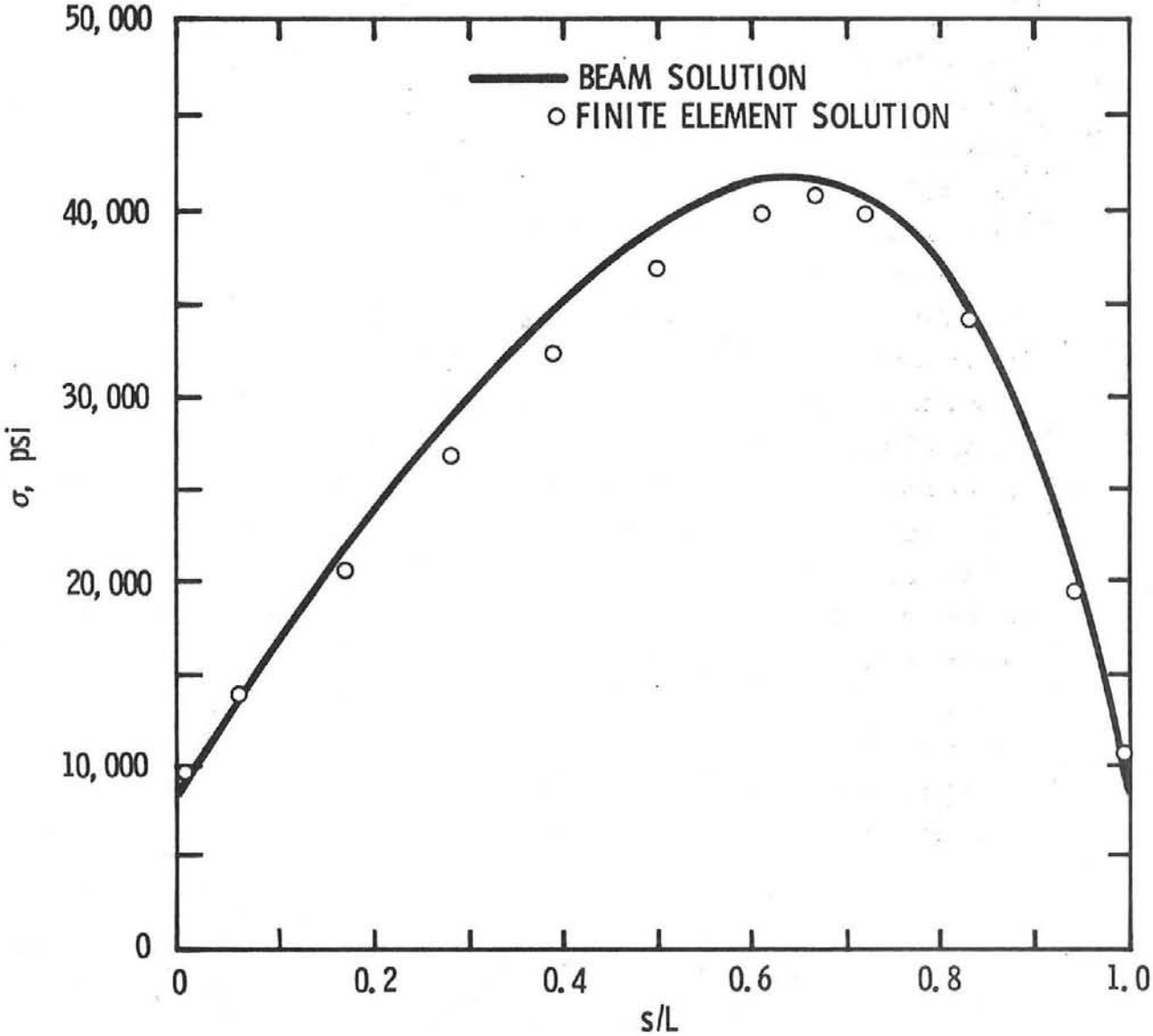

FIGURE 6. Comparison of Outer Fiber Meridional Stress, σ, vs. Meridional Coordinate, s/L.

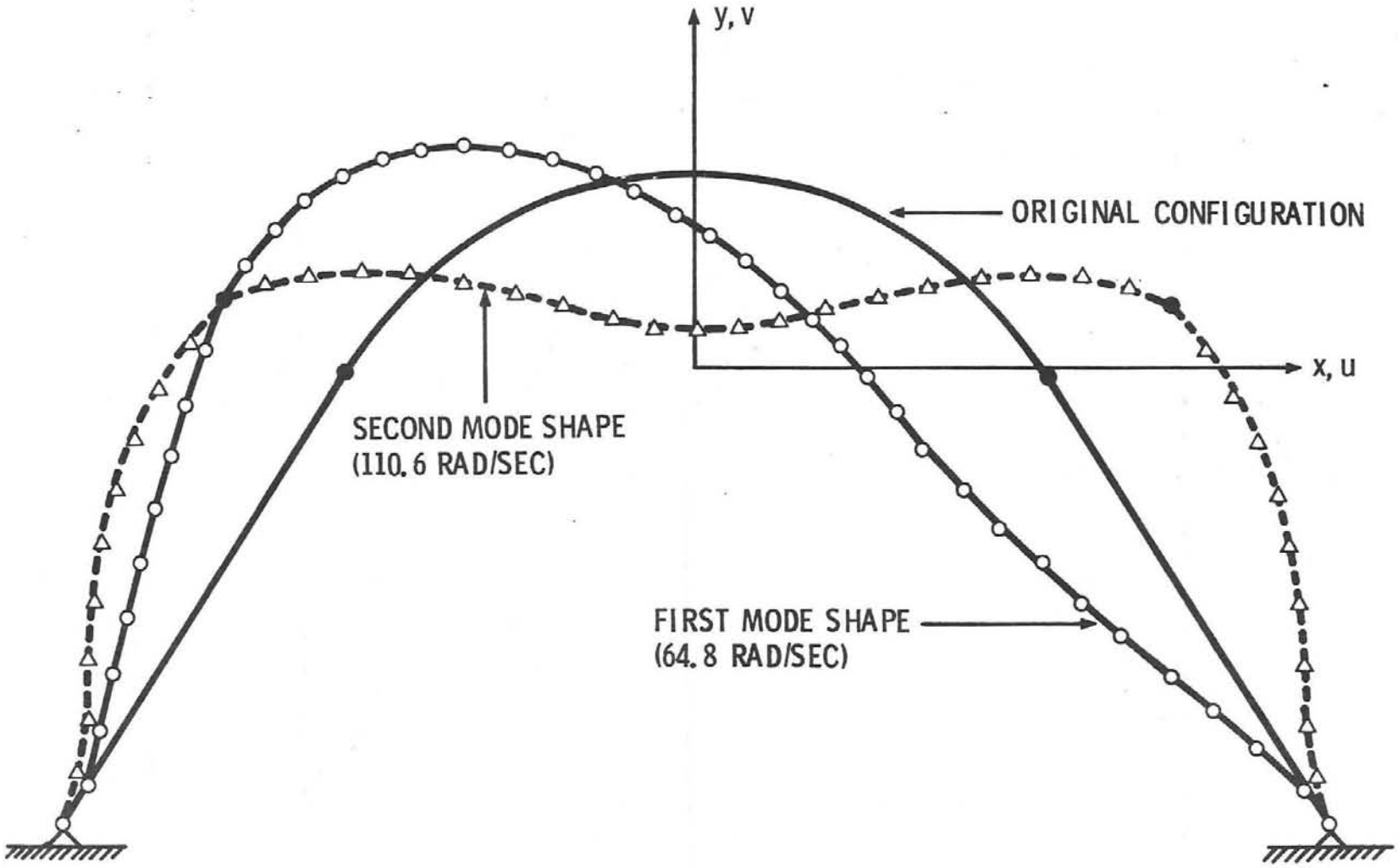

FIGURE 7. Blade Mode Shapes at Ω = 40 Rad/Sec.

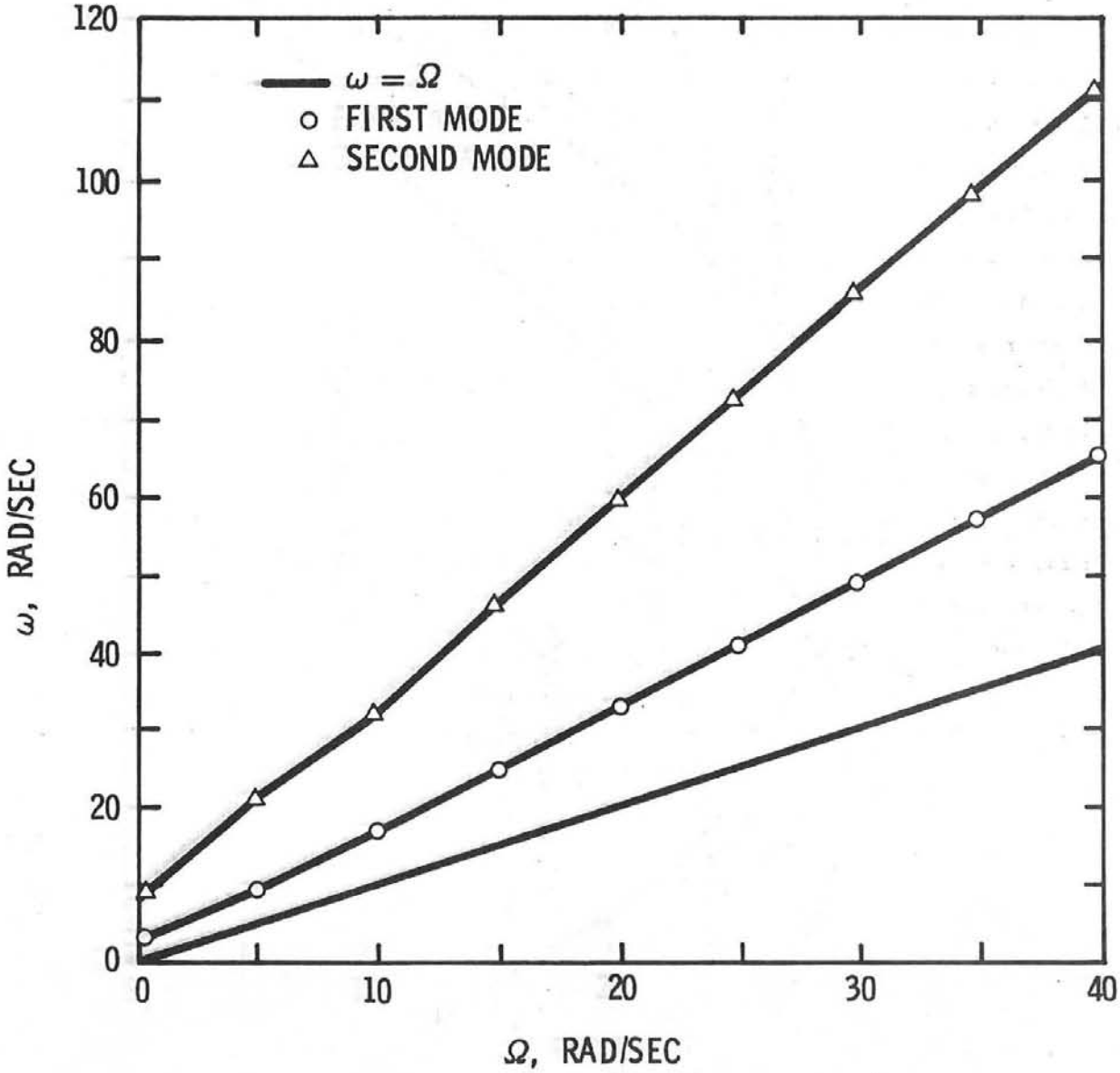

FIGURE 8. Natural Frequency Spectrum (First Two Modes), ω, vs. Angular Velocity, Ω.

Conclusions

The vertical-axis wind turbine has found favor throughout the United States and Canada as an alternative to conventional power sources. A method has been proposed here which should aid the designers of these vertical-axis systems, as well as designers of highly flexible, load-carrying structures, in general. The incremental loading procedure allows such flexible structures an opportunity to adjust their geometry to more efficiently resist subsequent loads. Although such procedures are difficult to apply to true tensile structures (e.g., cables and membranes), the modest bending stiffness of the turbine blades was sufficient to make them successful here. In addition, the ability to scan a portion of the natural frequency spectrum of flexible structures, at intervals during the application of load, should prove to be useful.

The results of both the nonlinear finite element analysis and the simplified beam analysis show that turbine blade stresses are significantly different between a troposkien shape and an alternate, more easily fabricated shape. These differences are manifested in slight amounts of inelastic deformation in regions of high bending stress intensity.

A logical and necessary extension of this work would be to include coupling effects between the wind-turbine tower and the rotating shaft.

References

[1] Blackwell, B. F., and Reis, G. E., "Blade Shape for a Troposkien Type of Vertical-Axis Wind Turbine," SLA-74-0154, Sandia Laboratories, Albuquerque, New Mexico (1974).

[2] McNamara, J. F., Incremental Stiffness Method for Finite Element Analysis of the Nonlinear Dynamic Problem, Ph.D. Dissertation, Brown University, Providence, R. I. (1971).

[3] McNamara, J. F. and Marcal, P. V., "Incremental Stiffness Method for Finite Element Analysis of the Nonlinear Dynamic Problem," in Numerical and Computer Methods in Structural Mechanics, ed. by S. J. Fenves, et al., Academic Press, Inc., New York, N. Y., pp 353-376 (1973).

[4] Hibbitt, H. D., Marcal, P. V., and Rice, J. R., "A Finite Element Formulation for Problems of Large Strain and Large Displacement," Int. J. Solids Structures, Vol. 6, pp. 1069-1086 (1970).

[5] Crandall, S. H., Engineering Analysis. A Survey of Numerical Procedures, McGraw-Hill Book Company, Inc., New York, p. 100 (1956).

[6] Jaeger, J. C., An Introduction to Applied Mathematics, Oxford University Press, London, P. 294 (1951).

Distribution:

J. Templin
Low Speed Aerodynamics Section
NRC-National Aeronautical Establishment
Ottowa 7, Ontario, Canada K1A056

A. Robb
Memorial University of Newfoundland
Faculty of Engineering & Applied Sciences
St. John's, Newfoundland
Canada A1C 5S7

H. Sevier
Rocket and Space Division
Bristol Aerospace Ltd.
P. O. Box 874
Winnipeg, Manitoba
R3C2S4 Canada

V.A.L. Chasteau
Dept. of Mechanical Engineering
The University of Auckland
Private Bag
Auckland, New Zealand

P. B. S. Lissaman
Aeroenvironment, Inc.
660 South Arroyo Parkway
Pasadena, CA 91105

O. Krauss
Div. of Engineering Research
Michigan State University
East Lansing, MI 48823

E. H. Phinney
Attn: P. A. Ekstrom
Atmospheric Sciences Department
Battelle-Pacific Northwest Laboratory
P. O. Box 999
Richland, WA 99352

W. Wiesner
Boeing-Vertol
P. O. Box 16848
Philadelphia, PA 19142

G. Herrera
Jet Propulsion Lab
4800 Oak Grove Drive
Pasadena, CA 91103

Michael Wahlig
Lawrence Berkeley Laboratory
Energy and Environment Division
University of California
Berkeley, CA 94720

Billy Hudson
Lawrence Livermore Laboratory
P. O. Box 808
Livermore, CA 94550

R. Muraca, MS 317
NASA Langley Research Center
Hampton, VA 23365

NASA Lewis Research Center
21000 Brookpark Road
Cleveland, OH 44135
Attn: J. Savino, MS 500-201

J. P. Taylor
National Academy of Engineering
2101 Constitution Ave. NW
Washington, D. C. 20418

Energy Research and Dev. Admin. (2)
1800 G Street NW
Washington, D. C. 20550
Attn: L. Divone
J. E. Rannels

E. Kist
Public Service Company
414 Silver Ave. SW
Albuquerque, N. M. 87102

B. Vance
Science Applications
1200 Prospect Street
LaJolla, CA 92073

Distribution (continued):

A. N. L. Chiu
Wind Engineering Research Digest
Spalding Hall 357
University of Hawaii
Honolulu, Hawaii 96822

Robert N. Meroney
Colorado State University
Dept. of Civil Engineering
Fort Collins, CO 80521

R. P. Vito
School of ESM
Georgia Tech
Atlanta, Georgia 30332

A. E. Van Antwerp
Ferris State College
Department of Physical Sciences
Big Rapids, MI 49307

Chumin Fu
Illinois Institute of Technology
Department of Physics
Chicago, Illinois 60616

New Mexico State University
P. O. Box 3450
Las Cruces, N.M. 88003
Attn: H. A. Daw
M. M. Sluyter
R. San Martin

Oklahoma State University
Stillwater, OK 74074
Attn: D. K. McLaughlin, ME Department

Oregon State University
Corvallis, OR 97331
Attn: R. Wilson, ME Department

Texas Tech University (2)
Lubbock, TX 79409
Attn: K. C. Mehta, CE Department
J. Strickland, ME Department

Robert G. Watts
Tulane University
Department of Mechanical Engineering
New Orleans, LA 70118

University of New Mexico (2)
Albuquerque, N.M. 87106
Attn: K. T. Feldman, Energy Research Ctr
B. Albrecht, ME Department

H. M. Busey
Division of Military Application
Hq., U.S. Energy Res. and Dev. Admin.
Washington, D. C., 20545

R. Beckman
Research and Design Institute
P. O. Box 307
Providence, R. I. 02901

B. Selby
5595 E. Arapaho
Boulder, Colo. 80303

Nevada Operations Office, ERDA (3)
P. O. Box 14100
Las Vegas, NV 89114
Attn: R. Ray, Operations (2)
H. Mueller, ARL

Los Alamos Scientific Laboratory
P. O. Box 1663
Los Alamos, NM 87544
Attn: R. R. Brownless, J-DO
J. R. Bartlit, P-8
J. D. Balcomb, Energy Division
R. Wagner, P-5

ERDA/ALO (3)
Kirtland AFB East, NM 87115
Attn: D. W. King
J. R. Cotton

1000 G. A. Fowler
1500 R. L. Peurifoy, Jr.
Attn: T. B. Lane, 1540
1541 S. W. Key
1542 T. G. Priddy
1543 H. C. Hardee
1544 R. T. Othmer
1544 W. N. Sullivan
1544 L. I. Weingarten (100)
4700 D. B. Shuster
4734 V. L. Dugan
Attn: J. Banas

Distribution (continued):

5000 A. Narath
Attn: J. K. Galt - 5100
E. H. Beckner - 5200
J. H. Scott - 5700
L. M. Berry - 5800
5600 A. Y. Pope
Attn: K. J. Touryan, 5640
5620 R. C. Maydew
Attn: E. C. Rightley, 5623
W. R. Barton, 5624
D. F. McVey, 5626
5623 L. V. Feltz
5625 H. R. Vaughn
5628 S. McAlees
Attn: B. F. Blackwell
R. E. Sheldahl
5710 G. E. Brandvold
5712 R. H. Braasch
Attn: E. G. Kadlec
A. F. Veneruso
5717 R. P. Stromberg
Attn: D. E. Randall
5840 D. M. Schuster
Attn: F. P. Gerstle, 5844
5844 B. L. Butler
6010 T. F. Marker
8000 T. B. Cook, Jr.
8100 L. Gutierrez
Attn: A. N. Blackwell, 8110
8266 E. A. Aas (2)
9483 W. V. Hereford
Attn: T. C. Looney
3141 L. S. Ostrander (5)
3151 W. F. Carstens (3)
For: ERDA/TIC (Unlimited Release)